Assimilation of lidar planetary boundary layer height observations

Andrew Tangborn, Belay Demoz, Brian Carroll, Joseph Santanello and Jeffrey Anderson

Response to reviews

Reviewer 1

Major comments:

1. L216-L225 and the assimilation impact from 00-08 UTC: I am confused why there appears to be exactly zero assimilation impact during the overnight hours. In Fig. 2, the forecast and analysis lines are exactly on top of each other for the first four verification times. However, looking at Figure 1, the innovation (observation minus background) can still be large during the overnight hours, especially for MYNN. For example, Fig. 1 shows MYNN underpredicting the PBLH by 300 m at 0400 UTC. Given that the error covariances at this time are also non-zero, as shown in Figure 7, I would expect at least some impact. Additionally, Fig. 2 shows the MYJ and MYNN RMS values of (T, Q, U, V) being exactly equal. This seems odd given that Fig. 1 shows them predicting very difference values of PBLH. Thus, I wonder if there is some error in the assimilation scheme or analysis techniques that could be leading to this appearance of zero-impact.

The analysis incremements are never zero, but are much smaller from 0-8 UTC. But we also found an inconsistancy in the definitions geopotential height and PBLH (the former defined above ground level and the latter above sea level), and have redone the assimilation. You can now see somewhat larger changes in some of the profiles during this time. Also, the smaller increments are also due to the variation in the lidar observation error estimates, which vary substantially during the day.

2. Figure 2: Given the large data gap between 08-22 UTC and the use of only six soundings for verification, I disagree with the use of a time-series to show the assimilation impacts. This choice leads to the appearance of the impact linearly increasing between 08-22 UTC, when it likely shows a very different shape in reality. Additionally, statements line L207 (water vapor mixing ratio has little impact until 22 UTC) are not correct given that there is likely an impact beginning at 12 UTC when the innovation becomes much larger. It is just that you do not have any radiosondes confirm that. I suggest removing this figure, or at least removing the lines that connect the verification times. I also suggest removing any text referring to temporal changes in the impacts C2

We have removed the lines between the radiosonde measurement times. It became difficult to see both of the PBL model forecasts without them, so we split Figure 2 into two figures (2 and 3). The text has been changed to reflect this.

3. Figures 3-6: These figures can be difficult to interpret given the lack of any innovation information. I found myself having to flip back and forth between these plots and Figure 1 to try and understand why the impacts were small at certain times. Please include the forecast PBLH on these figures, or at least annotate the innovation (Lidar PBLH minus forecast PBLH).

We have included the forecast PBLH in the profile plots.

4. Overly general writing: Sometimes I felt that the author's made general statements when those statements only were instead meant to refer to a specific PBL scheme. For example, it is stated in the abstract that assimilating PBLH observation improves water vapor relative to independent radiosondes. However, this does not appear to be the case for MYJ (figure 2). Additional examples of this are at L217, L228, L241, and L279. Please check and modify such statements throughout the manuscript.

The text has been changed to reflect the changes to assimilation (described in item 1 above), and to make the comments more specific. Though the L228 comment was concerning a plot that we didn't include. And L279 is a more speculative statement on how changing the state variables would be carried forward in time, though we have modified this to make it more qualified.

Minor comments:

L16 (and throughout): the use of "sonde" instead of "rawinsonde" or "radiosonde" feels a little informal. Please correct.

This has been changed.

L46: I suggest stating "non-local flux schemes" since that helps separate those types of schemes from the local TKE schemes.

done.

L50: The sentence beginning "These varying and distinct" is confusing. I suggest rewording.

It has been rewritten as: "The variety of definitions PBLH make it difficult to effectively evaluate existing models or develop new ones."

L58: I am not sure what the point of this reference to GPSRO is. This seems oddly specific and overly verbose. It could probably be removed.

Removed.

L73: Jumping from the discussion of ceilometers to lidars feels a little abrupt. Please improve the flow between these two paragraphs (i.e., stating something like "we use Doppler lidars as a proxy to determine the impact of assimilating PBLH from a network of ceilometers").

We have added further wording to make this transition less abrupt.

L74: Please provide a little more information on the brand and type of Doppler lidar used. There were multiple instruments employed during PECAN so it wouldn't hurt to be more specific.

This information has been added.

L81-L82 and L94-100: I suggest moving some of this content into the methodology sections. It doesn't really fit in an introduction.

We don't agree with making this move. These details are not about the assimilation algorithm, which is described in the methodology section. I don't think details about the observations belongs in methodology because the retrievals are not a part of the methodology developed in this work. Further, you are asking for more details about the lidar observations in this section already (L74 and L82). So it seems best to leave this the way it is.

L82: I would like to see more details on how PBLH is estimated from the Doppler lidar data instead of just giving the reference. This could provide needed context for understanding how different the estimates of PBLH are between the lidars, radiosondes, and the PBL parameterization schemes.

Additional description of the PBLH retrieval algorithm has been added.

Introduction: One thing I was curious about when reading this manuscript is the motivation for assimilating PBLH instead of directly assimilating the wind profiles collected by the lidars. Lidar wind profiles have been assimilated in the past with positive results shown (Kawabata et al. 2014, Degelia et al. 2020), so why go through the extra steps of deriving PBLH from those data? I suggest adding a sentence or two in the introduction to discuss this.

We have added "But we are interested assimilating the PBLH observations directly because the ceilometer network described above will focus on these retrievals, and satellite missions which measure PBLH are also planned.".

L116 and EnOI discussion: It seems that the EnOI computes the covariance structure with a spatial component (covariance over a given area). How representative is that of the EnKF method which can estimate covariance at a single point? Does that cause any issues with extrapolating these impacts to a hypothetical EnKF system (i.e., L269)?

We are only using the EnOI to compute covariance in the vertical direction, since we are concerned with the profile correction. With the EnKF one would also compute the horizonal structure as well. In addition, the variance estimate will dependend on the distance spacing of the profiles, with a larger distance resulting in a larger variance. We chose a relatively small set of 20x20 grid locations to minimize this effect. In the EnKF, one would also include inflation and horizontal localization. These would need to be worked out when an EnKF is constructed for this data type. We have added a couple of sentences on this.

L127: Is the same method used to compute PBLH for both the stable and convective boundary layer? I know MYNN is supposed to be more accurate at night compared to MYJ.

The PBLH estimate approaches are the same at all times. The values changed in this version as we found a inconsistency in the definition of PBLH, so now the MYNN scheme is more accurate during the night. We think the manuscript is reasonably clear on this.

L132: Please also list the grid-spacing for these simulations.

The grid spacing is 3km, and was already in the first version of the manuscript.

L111: Is there a reference for the NU-WRF forecasts run during PECAN?

The only reference at this point is Santanello, et al. 2019, which is an AGU meeting abstract.

L137-139: Is this true? I would expect that the covariance/correlation would be smaller when computed over a larger region?

Over a large region the meteorological conditions become more varied, so the variance becomes larger.

L148: Please include more information on the observation error variance! This term is equally as important in the analysis as the background error covariance. How is it determined? How do you convert the lidar wind errors into PBLH errors? Do you include any representation factors?

The PBLH observations are determined from the combined velocity variance dropoff, wind speed gradient and backscatter dropoff. The uncertainty is smallest where these values decay rapidly over a short distance. When the dropoff is more gradual (as in the morning), the estimated uncertainty is much larger. This is described in the text.

L151-155: It might be good to reference an EnKF paper for these approximations since it is the same technique applied here (i.e., Houtekamer and Zhang 2016).

Reference added.

L162: Please state the chosen value of α.

$\alpha = 8$ has been added to the paper.

L172-L179: Much of this paragraph detailing the model configuration is repeated from the methods paragraph beginning at L124. Please reduce.

We reduced the deails in the results section slightly.

L181: Is there a reference for the parcel method?

We added Holzworth, 1964.

L196: Why 800 hPa? Why not compute the RMS from the surface to the top of the PBL since you know its height? Please provide some justification for this number.

We chose $800mb$ because this is roughly the maximum height of the PBL on this day. If we chose to compute the RMS up to levels that vary with the PBLH, then it would be difficult to make direct comparisons between the RMS at different times in the day. We have added a sentence on this in the paper.

Figure 1: Should there be an additional sounding observation during the late evening? I only see five green triangles, but you reference six radiosonde launches. Additionally, there are six verification points shown in the time series plots.

The sixth radiosonde PBLH has been added to the figure.

L207: I recommend using absolute differences instead of percent changes.

We have changed this to absolute differences.

L213: I disagree with saying the assimilation reduces by the RMS "significantly". Is statistical significance computed here? Also, this sentence appears to be referring to the impact to U-wind in Fig. 2c, of which the impacts look extremely small to me.

We have changed the discussion here, and removed the term "significantly".

Figs. 2-6: Please add (a,b,c,d) headings to each figure to match the figure caption.

We changed the caption to read upper left, upper right, etc instead of using letters to identify the figure location.

Figure 2: I recommend changing (hour) in the x-axis to (UTC) to be consistent with the text. Also please be consistent between saying "U wind" and "zonal velocity" in the figure captions.

These have all been changed to "U wind".

L221-223, L276: I disagree with the statement of the model profiles "accurately" following the radiosonde profiles in Figs. 3-4. For example, the u-wind shows errors of 4 m/s, and the mixing ratio errors can be as large as 1-2 g/kg which is not exactly "accurate".

This has been changed so that the profiles are described as "more accurate" duing the early morning than they are in the late afternoon.

Figs. 3-6: I recommend reducing the vertical extent of these profiles you are primarily focusing on impacts within the PBL. Maybe 800 hPa since that is what you use for the RMS calculations?). Also, I notice that some of the axis labels and formats are different between these figures, so please be consistent.

We have kept the upper limit at about 600 mb because we felt it was important to show how the profile reveals the location of the top of the PBL (either the model or observation estimates), so it was helpful to include a region above the PBL. This also enables us to show how much correction is made above the PBLH. But we have made the fonts on the axis labels consistent.

L235-L38: I am not sure that the discussion of vertical localization fits with the rest of this paragraph.

We removed these two sentences. This had already been discussed in the methodology section.

L244: I do not understand this statement that suggests PBLH is more representative of water vapor flux. Please elaborate.

We removed the last two sentences from this discussion.

L279-282. There is a mix-up of tenses here. The first sentence uses present tense (the water vapor mixing ratio is over corrected), while the second sentence uses past tense (the assimilation corrected: : :). Please fix. I also noticed other instances of this so I recommend doing a pass to fix issues throughout the manuscript.

These sentences have been corrected.

Typos and wording changes

1. L5-6: Please spell out the affiliations.

Done.

2. L35-39: this sentence is overly long. Please split up or condense.

Done.

3. L42: Add a comma after "Alternatively".

Done.

4. L55: Please use UTC instead of "Z" time to be consistent with the rest of the paper.

Done.

5. L62: Change the reference to Hicks et al. 2016 to use parenthesis instead of brackets.

Done.

6. L114: The sentence beginning "Instead we use: : :" seems broken. Please fix.

Done.

7. L198: ntop is not used in this equation. Please remove.

Changed to $i = 8$.

8. L233: Fix the spelling for "independent".

Done.

9. L238: Please define "WV".

Done.

10. L267: Please change "assimilation" to "assimilating".

Done.

11. L288: Sentence beginning "The covariances" is broken. Please fix.

Done.

Reviewer 2

1. The definition of PBLH. As described on lines 77-82, for PBLH data calculation, the Doppler shift of the backscattered signal is used to calculate wind speed as a function of range, which can then be used to produce a multitude of wind and turbulence variables useful for PBL characterization (e.g. vertical velocity variance and signal-to-noise ratio variance). The PBLH algorithm applied for this study combines several such aerosol and wind variables for PBLH measurement and was described at length in Bonin et al. (2018). The PBLH in the model is estimated using the total kinetic energy (TKE) method. The two definitions are different but seem close enough. Is there a way to show to what extent the two PBLH definitions are comparable?

This Doppler lidar was not making measurements capable of direct TKE retrieval, only TKE proxies (such as vertical velocity variance), so an explicit apples-to-apples comparison is not possible here. To make further inference would be speculative, so instead we only present and discuss this best possible PBLH measurement from the Doppler lidar to assess model performance.

Once a much larger number of PBLH lidar observations are obtained, along with radiosonde observations, it would be worthwhile to generate some statistics on this, on both bias and random differences. We have 6 sonde observations to compare with our forecasts, and with these we can show here is how the lidar observations can impact the thermodynamic profiles within the PBL using assimilation of the lidar observations. With a better understanding of differences between the two PBLH schemes, and a much larger data set to compare with, it's likely that further improvements can be made.

2. The vertical localization factor. How is the parameter alpha in equation (6) chosen? According to the equation, this parameter works the same way for layers both above and below the PBL height, for example, if $k_PBLH = 4$, then C_loc at layer 3 is the same as C_loc at layer 5. However, that seems not the case in Fig. 5.

We have redone the assimilation to fix a couple of inconsistancies in the code, including this. The profile plots now show the vertical localization above and below the top of the PBL, though the final form of any localization that would be needed will be more clear once this is implemented with an enKF.

3. Equation (7). Where is number "8" coming from? The top of boundary layer is not a constant during the 22 hours, which can be seen clearly in Figures 3-6.

The maximum extent of the PBL in the late afternoon is at layer 8, and we felt is was more consistent to compare the same levels at each time, rather than comparing a much smaller number of layers during the night and early morning. This is explained further in the text.

4. In the abstract, it states that water vapor is improved by assimilating lidar PBLH. However, Fig. 5 shows that it is degraded.

We have corrected this statement. A more accurate statement is that the assimilation changes the water vapor profile in the right direction, but the increment is too large, so that the RMS difference with the radiosondes increases. This would require additional tuning in an EnKF.

Reviewer 3

1. Line 212 – ": : :.the assimilation reduces the RMS differences with sonde profiles significantly by 22 UTC for both models." From Fig. 2, the RMS difference of potential temperature, WVMR and V component of velocity have reasonable impact but there is little or no impact on U wind. Please correct the statement if it was a mistake, or, if not, please elaborate how the impact is significant. Also please adjust the Y axis limits of V wind to the same as that of U wind.

We have made some changes here due to changes in the solution in this revision. Please see the response to the last item from reviewer 2. We have made the y-axis limits the same for the U and V plots.

2. In Figs. 3 and 4 both analysis and forecasts profiles of potential temperature, WVMR and velocities, U and V, coincide each other at 4 UTC. However, in Fig. 1, the PBLH at 4 UTC is not the same for MYNN forecast although MYJ forecast PBLH has the same value as the radiosonde. The PBLH difference of MYNN forecast to radiosonde is around 300 m from Fig. 1 which creates a doubt regarding Fig. 4 (MYNN scheme) at least if not Fig. 3. May be the innovation was not large enough to create an impact in the assimilation system. Also another reason for doubt is due to the significant magnitude of covariance of PBLH with the variables for 4 and 8 UTC. Hence, I would suggest the author to create the same Figs. 3 and 4 with an additional background profile (may be use a dashed line of the same colour) for each of the variables to remove the doubt.

We have made some corrections to the code, which has changed both the innovations and the corrections to the profiles. We have also put the lidar observation levels (in pressure) on the profile plots to make more lear the magnitude of the innovations. There are now some what larger corrections to the profiles in the early morning, and none of them is zero.

Minor Comments:

1. I would suggest the author to include a brief description of Doppler lidar just after the ceilometers. A brief description on the pros and cons of Doppler lidar (with references to the system used) and how it is superior to ceilometers could be added.

We have added further details on the Doppler lidar.

2. Line 134 - Please add some more details regarding the assimilation design in the methodology section. The sentence ": : :experiments are all less than 24 hours from the most recent global analysis" is not clear enough for readers. Line 98 - "The assimilation is done on 22 hourly WRF forecast fields: : :" may be omitted or modified after the above addition in the methodology section.

We have added further explanation as to where the forecasts start (0 UTC) from the NOAA global forecast system (GFS) with a final initialization at 0 UTC.

3. Line 178 – Radiosonde launches were 6 times in total. The reader understands MYJ has 5 radiosonde comparisons since it stopped at 22 UTC whereas MYNN has 6 radiosondes. Please clarify this point.

The missing radiosonde has been added to the PBLH plot.

Typos and corrections:

1. Line 59 – "Wulfmeyer et al. 2015" not found in the reference section.

Added.

2. Line 67 - Please check "Brooks, 2003". I could not find the reference in the reference section.

Added.

3. Line 144 – The sentence "Instead we use: : :error statistics" should be corrected.

We have changed this sentence, but we think you had meant line 115.

4. Line 119 – "We use profiles from: : :" feels like repetition from line 115.

We think you meant line 144 here. And we have shortened and simplified the sentence to avoid repetition.

5. Line 129 – Please describe "W".

W is the vertical velocity, but we are not showing it here because there are not observations to validate it. So we have removed it.

6. Line 220 – Please change "plue" to "blue".

Done.

7. Line 244 – "Demoz et al 2006; Crook, 1996" could not be found in the reference section.

These citations have been added to the reference list.

8. Line 272 – "an" is used twice, please correct.

Done.

9. The following references were found in the reference section without citation in the manuscript. Please cite these wherever necessary.

"Banks, R. F., J. Tiana-Alsina, F. Rocadenbosch, and J. M. Baldasano (2015) Performance evaluation of the boundary-layer height from lidar and the Weather Research and Forecasting Model at an urban coastal site in the north-east Iberian Peninsula. Bound.-Layer Meteor., 157, 265–292, https://doi.org/ 10.1007/s10546-015-0056-2."

"Cohen, A.E., S.M. Cavallo, M.C. Coniglio and H.E. Brook (2015), A Review of Planetary Boundary Layer Parameterization Schemes and Their Sensitivity in Simulating Southeastern U.S. Cold Season Severe Weather Environments, Wea. Forecat., 30, 591-612."

"Tucker, S.C., S.J. Senff, A.M. Weickmann, W.A. Brewer, R.M. Banta, S.P. Sandberg, D.C. Law and R.M. Hardesty (2009), Doppler Lidar Estimation of Mixing Height Using Turbulence, Shear, and Aerosol Profiles, J. Atmos. Ocean Tech., 26, 673-688."

These References have been removed.

Assimilation of lidar planetary boundary layer height observations.

Andrew Tangborn[1], Belay Demoz[1,2], Brian J. Carroll[2], Joseph Santanello[3]and Jeffrey L. Anderson[4]

[1]Joint Center for Earth Systems Technology, University of Maryland Baltimore County, Baltimore, MD, USA

[2]Dept. of Physics, University of Maryland Baltimore County, Baltimore, MD, USA

[3]Hydrological Sciences Laboratory, NASA Goddard Space Flight Center, Greenbelt, MD, USA

[4]National Center for Atmospheric Research, Boulder, CO, USA

Corresponding author: Andrew Tangborn, `tangborn@umbc.edu`

Abstract

Lidar backscatter and wind retrievals of the planetary boundary layer height (PBLH) are assimilated into 22 hourly forecasts from the NASA Unified - Weather and Research Forecast (NU-WRF) model during the Plains Elevated Convection Convection at Night (PECAN) campaign on July 11, 2015 in Greensburg, Kansas, using error statistics collected from the model profiles to compute the necessary covariance matrices. Two separate forecast runs using different PBL physics schemes were employed, and comparisons with ~~5 independent sonde~~ 6 independent radiosonde profiles were made for each run. Both of the forecast runs accurately predicted the PBLH and the state variable profiles within the planetary boundary layer during the early morning, and the assimilation had ~~little~~ a small impact during this time. In the late afternoon, the forecast runs showed decreased accuracy as the convective boundary layer developed. However, assimilation of the doppler lidar PBLH observations were found to improve the temperature ~~, water vapor and~~ and V velocity profiles relative to independent ~~sonde profiles.~~ radiosonde profiles. Water vapor was over corrected, leading to an increased differences with independent data. Errors in the U velocity were made slightly larger. The computed forecast error covariances between the PBLH and state variables were found to rise in the late afternoon, leading to the larger improvements in the afternoon. This work represents the first effort to assimilate PBLH into forecast states using ensemble methods.

1 Introduction

The planetary boundary layer (PBL) plays an important role in both weather and climate. This layer is where the Earth's surface interacts with the atmosphere, exchanging heat, moisture and pollutants. The PBL height (PBLH) is central to these interactions and is controlled by the energy flux from the surface. Under certain conditions during daytime it defines the convective boundary layer (CBL) and during nighttime it is the stable (non-convective) boundary layer (SBL). Trace gases and aerosols emitted from the surface are rapidly transported within this layer by turbulent atmospheric motion, and transfer of energy and mass into the free troposphere occurs across an interfacial layer at the top of the PBL. The PBLH is fundamental to weather, climate, atmospheric turbulence and pollution through its role in land-atmosphere interactions and mediation of Earth's water and energy cycles (Santanello et al. 2018)~~and its impact on~~ . It affects convection in the troposphere, which is generally initiated within the boundary layer and then penetrates the top (Hong and Pan, 1998; Browning, et al. 2007). Thus, accurate knowledge of the PBLH is essential for both weather, pollution and climate forecasting.

The PBLH is defined by thermodynamic properties such as a temperature inversion or hydrolapse which can be measured by radiosonde. Alternatively, the drop off in aerosol concentration that occurs across the top of the PBL is used, since aerosols are well mixed throughout the PBL (Hicks, et al., 2019). Atmospheric models rely on parameterization schemes to define the structure of the PBL and compute PBLH. These are generally either local mixing schemes that use local turbulent kinetic energy (TKE, Janjic, 1994) or non-local flux schemes (Hong and Pan, 1996). Generally, these PBL parameterizations have systematically higher PBLH relative to observed values (Hegarty et al., 2018), and also have difficulties modeling the growth of the convective layer during the morning. ~~These varying and distinct~~ The variety of definitions of PBLH ~~across models and observations remain a challenge in terms of utilizing both for process understanding or model evaluation/development~~make it difficult to effectively evaluate existing models or develop new ones.

Observations of PBLH are traditionally made by radiosonde measurements, which have high vertical resolution but are expensive to launch frequently and are thus limited to special experiments and/or ill-timed launches (*e.g.* 00/~~12Z~~ 12 UTC National Weather Service launches) with respect to ~~the~~ convective and stable PBL development. Likewise, spaceborne measurements of the lower troposphere from passive and active instruments ~~(with the exception of Global Positioning System Radio Occultation (GPSRO), Ao, et al. 2008)~~ are severely limited in vertical, spatial, and/or temporal resolution (Wulfmeyer et al. 2015). Ground based measurement of PBLH has been proposed for an extensive network of ceilometers by adding to the functionality of instruments that were designed for measuring cloud heights (Hicks et al., 2016). The ceilometer measures the time required for a laser pulse to return to a receiver, from which the height of the scattering is determined. The intensity of the backscatter is correlated with the density of aerosols at a given height and the PBLH is inferred from the location of the maximum negative gradient of the backscatter intensity. Several algorithms employ wavelet transforms to identify the location of the negative gradient (e.g. Brooks, 2003; Knepp, *et al.*, 2017)~~, which relies on finding the wavelet dilation that is large enough to be distinct from noise and small-scale gradients in the backscatter profile~~. This existing network of ceilometers could be used to create a relatively dense network of frequent PBLH observations, as was recommended by the 2009 study from the National Research Council (NRC, 2009) and the Thermodynamic Profiling Technologies Workshop (NCAR, 2012).

~~The lidar observations used in this study were taken~~ Since the ceilometer PBLH observations were not yet available for the campaign we are using, we employ doppler lidar observations made at the PECAN site in Greensburg, Kansas, to demonstrate the methodology. The data is from a ~~commercial~~ Leosphere WINDCUBE-200S Doppler lidar owned and operated by the University of Maryland, Baltimore County (Delgado et al., 2016). This lidar operates at an infrared wavelength, and hence receives its strongest backscattered signal within the aerosol-laden PBL and is often below the measurement noise floor above the PBL. The Doppler shift of the backscattered signal is used to calculate wind speed as a function of range, which can then be used to produce a multitude of wind and turbulence variables useful for PBL characterization (e.g. vertical velocity variance and signal-to-noise ratio variance). While Doppler lidars and ceilometers are similar in aerosol detection, a Doppler lidar's additional wind measurement capability makes it more broadly applicable and at times more accurate than a ceilometer for PBLH measurement. The PBLH algorithm applied for this study combines several such aerosol and wind variables for PBLH measurement~~and was~~. Each PBLH retrieval involves measurement of turbulence intensity, horizontal wind profiles and backscatter intensity. The heights of steep gradients in these quantities are determined using empirical thresholds and wavelet transform techniques, and the three estimates are combined using fuzzy logic. This is described at length in Bonin et al. (2018). Additional lidar parameters and the application of the algorithm to PECAN data were presented in Carroll et al. (2019). ~~Each PBLH measurement was~~ The PBLH measurements were made from a repeating 25-minute lidar scan cycle. This Doppler lidar and PBLH algorithm combination are generally well-suited for accurate and precise measurement of the PBLH during the daytime boundary layer, nocturnal boundary layer, and morning transition period (Bonin et al. 2018, Carroll et al. 2019). The evening transition is the most challenging for this setup due to due to difficulties in defining a clear mixing layer during the decay of a turbulent daytime PBL (Lothon et al. 2014).

The question remaining is how to assimilate these observations into a numerical weather prediction (NWP) model. ~~PBLH~~ A number of studies have explored assimilating thermodynamic profile measurements from lidar (Hu et al. 2019, Coniglio et al. 2019, Degelia et al. 2019) and have shown that this increases the accuracy of model PBLH estimates.

But we are interested assimilating the PBLH observations directly because the ceilometer network described above will focus on these retrievals, and satellite missions which measure PBLH are also planned. PBLH is a diagnostic variable in NWP parameterized physics models. This means any correction to PBLH will be lost during the model forecast unless the PBLH height observation is used to correct state variables such as temperature and moisture. This could be done either by creating an adjoint of the PBL parameterization scheme, or through the use of an ensemble Kalman filter which would determine the error covariances between PBLH and state variables in the model. The structure of the covariance, and how the state variables are changed by assimilating PBLH, will depend on which PBL scheme is used. We will show how such a system could work by conducting a posteriori lidar PBLH observation impact experiments using forecast fields from a NASA Unified - Weather and Research Forecast (NU-WRF, Lidard-Peters, 2015) model runs for one day during the Plains Elevated Convection at Night (PECAN) campaign on July 11, 2015. The assimilation is done on 22 hourly WRF forecast fields throughout the day without cycling the analysis fields back into the model~~with ~~, using two different PBL parameterizations. In this paper, we demonstrate a new and promising method that uses the ~~relative ~~lidar-based aerosol backscatter and wind derived PBLH to correct model forecasted state variables. The purpose here is to show how ensemble computed error covariance can transfer observational information from PBLH to the state variable profiles.

2 Methodology

The assimilation methodology is based on the ensemble Kalman filter (EnKF)(Evensen, 2009), where the analysis state is the estimate with the minimum estimated errors, relative to the given error statistics. It differs from the EnKF in that the analysis is not used as an initial state for the next model forecast. Rather, two existing one day NU-WRF forecasts, with different PBL physics schemes, are used when lidar measurements are available at a single location. These forecasts were produced as a part of the PECAN campaign in 2015, and we resuse them here to demonstrate the assimilation algorithm that we have developed. These were not ensemble forecasts so we cannot build a standard ensemble Kalman filter from them. Instead we use Ensemble Optimal Interpolation (EnOI), ~~we use ~~in which profiles from neighboring model gridpoints ~~to obtain and~~ are used to obtain an estimate of error statistics (Oke, *et al.*, 2010; Keppenne, *et al.*, 2014).

This approach will allow for the construction of the vertical component of covariance, which is needed in order to understand how PBLH can be used to correct atmospheric profiles through the use of profile and PBLH statistics. We use profiles from nearby model grid points and have tested the system with varying numbers of grid points in the ensemble. An ensemble Kalman filter would likely give different covariance information, but the basic relationship between the state variable profiles and the PBLH are determined by the model in the same manner here.

The two NU-WRF simulations use the Mellor–Yamada–Janjic (MYJ)[Mellor and Yamada, 1974, 1982; Janjic, 2002] and Mellor-Yamada-Nakanishi-Niino level 2.5 (MYNN) [Nakanishi and Niino, 2009] which are local 1.5 and 2.5 order turbulence closure schemes respectively. The PBLH in each of these models is estimated using the total kinetic energy (TKE) method. The NU-WRF forecast state variables are temperature (T), moisture (Q) and velocity (U,V), and we define the forecast vector $\mathbf{x}^f = [T^f \; Q^f \; U^f \; V^f \; (PBLH)^f W^f \;]$ $\mathbf{x}^f = [T^f \; Q^f \; U^f$ where we have combined PBLH with the state variables to enable the covariance calculation between them. The forecast runs are initiated from a global the NOAA global forecast system (GFS) reanalysis interpolated to the local domain of 30-48N and 84-110 W, with 220×220 lat/lon and 54 vertical levels. Therefore the state at the initial time , at 0 UTC. At this time, the initial state has assimilated all of the convential and satellite observations globally. This means that our experiments are all less than 24 hours from the most recent global analysisThe two WRF forecast experiments start at 0 UTC, and are run for 22 and 23 hours for the MYJ and MYNN experiments, respectively. We use an ensemble of the 20×20 nearest gridpoints, so that all of the ensemble members are within about 30 km of the lidar observations (since the grid spacing is about 3 km). Generally, larger ensembles using gridpoints farther away will result in larger forecast error covariance because the geographic variability. So this ensemble size was chosen as a balance between ensemble size and geographic localization. The forecast standard deviation for PBLH on the chosen ensemble was around 27 m at 22 UTC.

The forecast error covariance, $\mathbf{P}^f$ is defined as

$$\mathbf{P}^f = \left\langle (\mathbf{x}^f - \mathbf{x}^t)(\mathbf{x}^f - \mathbf{x}^t)^T \right\rangle \tag{1}$$

where the summation is over the grid points $i = 1, N_{lon}$, $j = 1, N_{lat}$ and $\mathbf{x}^t$ is the (unknown) true state, on the discrete model grid. We only assimilate the observation $y^o = PBLH = H(\mathbf{x}^f)$ where H is the non-linear observation operator. The analysis equation is

$$\mathbf{x}^a = \mathbf{x}^f + \mathbf{K}(y^o - H(\mathbf{x}^f)) \tag{2}$$

where the gain matrix, $\mathbf{K}$ is defined by:

$$\mathbf{K} = \mathbf{P}^f\mathbf{H}^T(\mathbf{H}\mathbf{P}^f\mathbf{H}^T + (\sigma^o)^2)^{-1}, \tag{3}$$

σ^o is the observation error standard deviation supplied with the lidar retrievals, and is determined from the combined uncertainty of the vertical velocity variance, velocity gradient and backscatter gradient. Generally, when these quantities change rapidly at the top of the PBL, then the estimated error is small. The error estimates are larger when (during the evening), the gradients are much more gradual. $\mathbf{H}$ is the linearized observation operator for PBLH. Because the PBLH is related to the state variables via the two PBL physics schemes, determining $\mathbf{H}$ would require linearizing the PBL physics at every analysis time. ~~Instead of this approach,~~ Rather, here we use the ~~ensemble of profiles from the forecast field locations $\mathbf{x}^f$ and the boundary layer heights $PBLH^f$ to obtain the ensemble estimates~~EnOI described above to get:

$$\mathbf{P}^f\mathbf{H}^T \approx \left\langle (\mathbf{x}^f - \mu_{\mathbf{x}}{}^f)\ (H(\mathbf{x}^f - \mu_{\mathbf{x}}{}^f))^T \right\rangle \tag{4}$$

and

$$\mathbf{H}\mathbf{P}^f\mathbf{H}^T \approx \left\langle H(\mathbf{x}^f - \mu_{\mathbf{x}}{}^f)\ (H(\mathbf{x}^f - \mu_{\mathbf{x}}{}^f))^T \right\rangle \tag{5}$$

where $\mu_{\mathbf{x}}{}^f$ is the mean forecast state of the ensemble of profiles. See Houtekamer and Zhang (2016) for a review of ensemble Kalman filter techniques.

We expect the correlation between the airmass within the PBL and the free troposphere to drop away rapidly, because of limited intereactions between them. We found that this can cause errors in the analysis profiles if error covariance and PBLH is allowed to continue into the troposphere. To reduce these errors we have added an exponential decay starting at the model level closest to the PBLH (k_{PBLH}) to define a vertical localization factor:

$$C_{loc} = exp\left[-\alpha(\frac{k - k_{PBLH}}{k_{PBLH}})^2\right] \tag{6}$$

where k is the model level and ~~α~~ $\alpha = 8$ is an experimentally determined factor. This ensures that the covariance between the PBLH and the state variables becomes small within a couple of model levels into the free troposphere.

This system is solved at each hour using the nearest lidar profile ~~observations~~ observation in time, and the resulting analysis fields are compared to ~~sonde~~ radiosonde profiles when the latter are also available. There are 22 or 23 analyses (for each forecast run), and ~~5~~ 6 times where comparison with ~~sonde~~ radiosonde profiles are made. We focus on the impact of the assimilation on the state variables T, Q, U and V rather than the PBLH because only the state variables would be retained by a forecast.

3 Results

The NU-WRF simulations, taken from existing forecast runs used for the PECAN campaign (Santanello *et al.*, 2019) are initialized using a National Center for Environmental Prediction (NCEP) Global Forecast System (GFS) reanalysis~~interpolated to the domain 30-48N and 84-110 W, with 54 vertical levels~~. The two forecast runs were conducted using MYJ PBL physics (2-22 UTC) and MYNN (2-23 UTC) on July 11, 2015. Lidar PBLH observations were made every 25 minutes on that day in Greensburg, KS (37.6 N, 99.3 W), while balloon soundings were launched from that location 6 times as part of the Plains Elevated Convection At Night (PECAN; Gerts et al. 2017). Figure **??** shows the PBLH during that day~~and~~ , derived from the two NU-WRF forecasts, lidar observations and soundings. We have determined the sounding PBLH using the parcel method ~~,~~ (Holzworth, 1964), which defines the top as the height where the potential temperature first exceeds the ground temperature. The lidar PBLH (black *, derived using the method reported in Bonin, 2018) closely matches the ~~sonde~~ radiosonde estimates (green triangles) in the late evening to early morning (2-7 UTC), while it is somewhat lower in the afternoon. The two NU-WRF forecasts differ from the observations depending on the time of day. In the early morning and early afternoon the MYJ forecasts (red triangles) ~~are slightly~~ both are higher than the observations, then ~~fall behind the rise seen in~~ rise less than the lidar observations ~~(~~in the late morning and early afternoon (12-17 UTC, there are no ~~sonde~~ radiosonde measurements to compare to here) before rising much higher than the observations in the late afternoon ~~. The MYNN forecasts (blue squares)are lower than the observations from early morning until early afternoon before rising higher (but not as high as MYJ)~~(18-24 UTC).

Since we are primarily interested in the impact of the assimilation on state variables within the boundary layer, in ~~Figure ??~~ Figures **??** and **??** we plot the RMS dif-

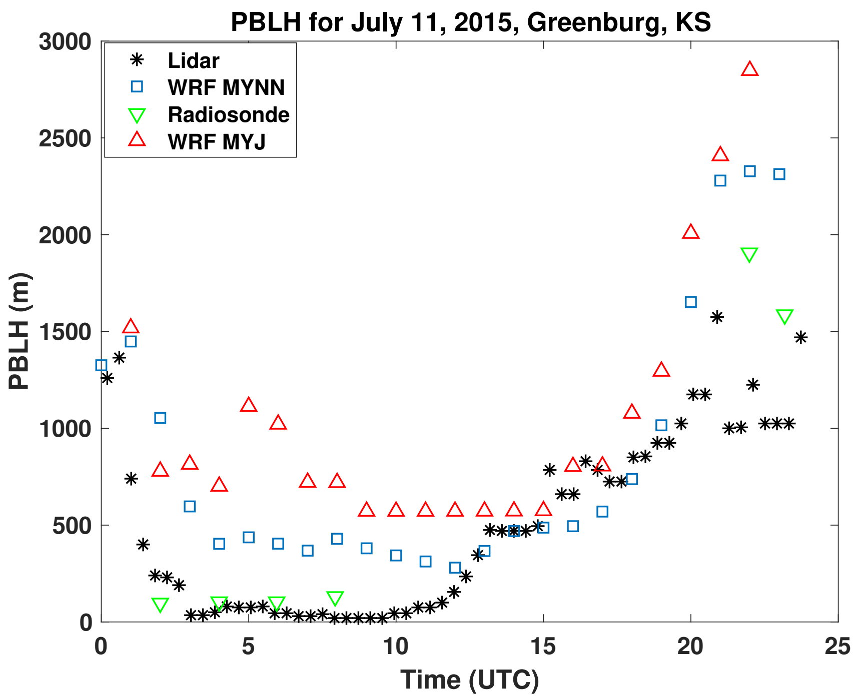

c

Figure 1. PBLH vs UTC time for July 11, 2015 for lidar backscatter (black *), WRF model - MYJ (red triangles), ~~sonde observations using parcel method (green triangles) and~~ WRF model - MYNN (blue squares), and radiosonde observations using parcel method (green triangles).

ference between the model and the independent (unassimilated) ~~sonde~~ radiosonde profiles from the surface to roughly the top of the boundary layer ~~(~~in the late afternoon. This corresponds to the first 8 ~~levels~~layers, or about 800 mb~~). So for the~~. We use a fixed number of layers so as to make the comparisons of the RMS differences consistent during the day, rather than computing the RMS over a different number of layers as the PBL grows during the day. For the temperature forecast, the RMS difference would ~~be~~ is

$$RMS(t_a) = \left[\frac{1}{8} \sum_{i=1}^{8} (T_i^f - T_i^{sonde})^2 \right]^{1/2} \qquad (7)$$

where t_a is the analysis time and ~~$ntop$~~ $i = 8$ is the model level at the top of the PBL ~~.~~ ~~Figure ?? shows~~ in the late afternoon. Figures **??** and **??** show the RMS differences with the ~~sonde~~ radiosonde profiles throughout the day for the forecasts (blue x) and analyses (red squares) for potential temperature (~~a~~upper left), water vapor mixing ratio ~~(b~~WV (upper right) and the U (~~c~~lower left) and V (~~d~~lower right) components of velocity. ~~The MYNN profiles are shown by solid lines while the MYJ profiles are dashed lines.~~

During the night (2-9 UTC), the assimilation has ~~very little~~ a relatively smaller impact on the potential temperature RMS differences (upper left) in the early morning (6 and 8 UTC), and the two forecasts have similar accuracy. By late afternoon (22 and 23 UTC, note that the MYJ forecast stops at 22 UTC) the ~~sonde~~ radiosonde comparisons show that the assimilation reduces RMS differences in the potential temperatures by ~~nearly 50% for MYNN and around 80% for MYJ~~ around $1.5K$ for MYJ and $2K$ for MYNN. The water vapor mixing ratio (~~b~~upper right) also has little impact from the assimilation ~~until 22 UTC, and then the~~ between 2 and 8 UTC, but at 22 UTC (the next radiosonde profile) the RMS difference for ~~the MYJ analysis more than doubles whereas it decreases by roughly half for MYNN. The forecasts for the 2 schemes show about the same differences with the sonde moisture profiles throughout the day~~both MYJ and MYNN analysis increase by at least $1.5 \times 10^{-3} kg/kg$ in the late afternoon. The U-velocity profiles (~~c) begin to show~~ lower right) show small differences between the MYJ and MYNN ~~by~~ through 8 UTC (3 a.m. local time) and the assimilation ~~reduces~~ increases the RMS differences with ~~sonde profiles significantly by~~ radiosonde profiles by nearly $1m/2$ starting at 22 UTC for both models. The V-velocity profiles (d) begin to differ between MYJ and MYNN for the forecasts at 8 UTC ($0.5m/2$ decrease), and assimilation ~~reduces~~ also decreases the RMS differences with ~~sondes~~ radiosondes in late afternoon by ~~10-20%~~$1.5 - 2m/s$.

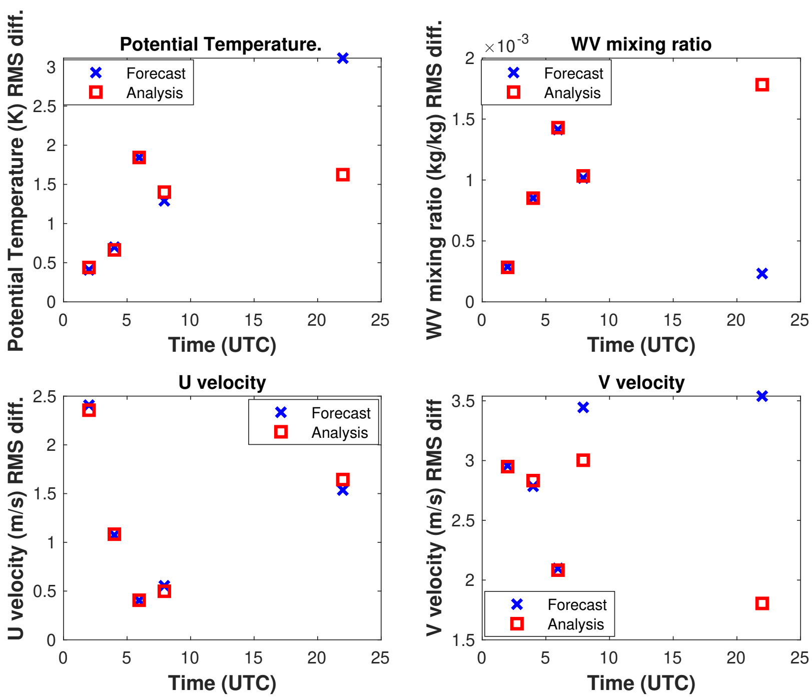

Figure 2. RMS difference ~~from surface to top of PBL~~ for lowest 8 layers, vs. time of forecast (blue x) and analysis (red square) with ~~sonde~~ radiosonde profiles for ~~(a)~~ potential temperature ~~,~~ (~~b~~upper left), water vapor ~~,~~ (~~c~~upper right)~~zonal~~ , U velocity ~~and~~ (~~d~~lower left) ~~meridional~~ and V velocity (lower right).~~The solid lines are for the MYNN PBL model and the dashed lines are for the MYJ PBL model. Times shown are UTC.~~

.1in

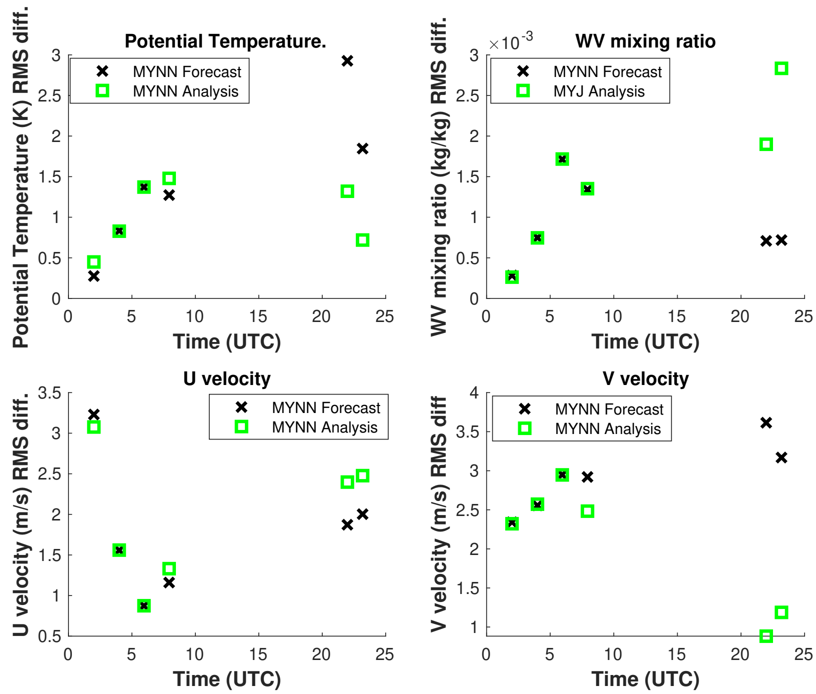

Figure 3. Same as Figure ??, but for MYNN PBL model, with forecast (black x) and analysis (blue square).

.1in

We would like to understand why there is ~~no data~~ a smaller impact during night time and early morning, whereas there ~~is overall improvement in~~ are decreases inthe RMS differences in temperature and V velocity and increases in moisture and U velocity in the late afternoon. To this end, we plot the forecast, analysis and ~~sonde~~ radiosonde profiles (T, Q, U and V) at 4 UTC (11 p.m. local time) and 22 UTC (5 p.m. local time) in Figures **??**-**??**. At 4 UTC, (Figures **??**,**??**) these clearly indicate that there ~~is no correction~~ are small corrections made by the assimilation, as the red and ~~plue profiles coincide~~blue profiles closely overlap. But it also shows that the profiles (particularly temperature and moisture) more accurately follow the ~~sonde profiles~~ radiosonde profiles (except for the U velocity above the PBL), meaning that there is ~~little~~ less room for improvement to the forecast state. ~~This is consistent with the PBLH forecasts in~~ In contrast, Figure (**??**) ~~,~~ ~~which shows that little difference between the forecast~~ shows that the forecast PBLH (particulary MYJ) ~~and lidar observation is very small~~is quite a bit higher than the lidar observation at 4 UTC. In the late afternoon (Figures **??**, **??**) ~~show~~ indicate that there are large differences ~~forecast~~ between the forecast and ~~sonde~~ radiosonde profiles for all of the state variables, and the forecast PBLH values differ substantially from the lidar measurements as well. The correction to to the ~~profiles is generally in the correct direction, indicating that the forecast error covariance from the ensemble can relate the PBLH to the state variables.~~ forecast profiles generally pushes the analyses towards the independent radiosonde profiles, particularly for temperature and V velocity.

So the forecasts that ~~accurately~~ that predicted both PBLH and state ~~variable profiles~~ variables with relatively greater accuracy in the early morning were not corrected, while the less accurate afternoon forecast was drawn towards the independent ~~sonde~~ radiosonde measurements. The assimilation also made changes to the vertical velocity (W) in the afternoon, but there is no ~~indpendent~~ independent data to compare with so we have not included it.

~~Initial experiments without vertical covariance localization (not shown) found that the analysis profiles were changed substantially well into the troposphere, which increased the RMS differences with the sonde profiles there. With the addition of the vertical correlation the analysis profiles relax back to the forecast in the troposphere.~~ The WV profile is shown to be increased by the assimilation (since WV and PBLH are negatively correlated and higher PBLH corresponds to lower WV levels in the PBL models), but the analysis overshoots the ~~sonde~~ radiosonde WV profile, hence causing the increase in the water vapor RMS difference in ~~Figure ??(b)~~Figures **??** and **??**. Compared to temperature, WV is highly variable in time and space and it has been shown in the past that slanted balloon trajectories under estimate the WV present (Demoz et al 2006; Crook, 1996). The ~~PBLH may be a macroscale observation that is forcing a correction to the WV flux and hence pointing out an issue in measurements. Future studies should look at the profile measurements of WV from lidars. The two components of velocity (c, d) are both drawn towards the sonde profiles, but by more modest amounts~~U velocity difference with the radiosonde is larger for the analysis, but this correction is more difficult because the differences (at least for MYJ) are both positive and negative and the PBLH observation only contains a single piece of information. The V velocity is, on the other hand, greatly improved by the assimilation. These analysis profiles in show that, for this one analysis time, the assimilation is pushing the state variables in the proper direction for temperature, V velocity and moisture, though the moisture correction overshoots the readiosonde profile. The reason for these corrections to the state variable profiles is that the error covariance between PBLH and each state variable, $\mathbf{P}^f\mathbf{H}^T$, can be computed from the ensemble of profiles that was collected from the model grid. The forecast PBLH for each profile was computed using the full PBL physics, and therefore contains the essential correlation information between these variables.

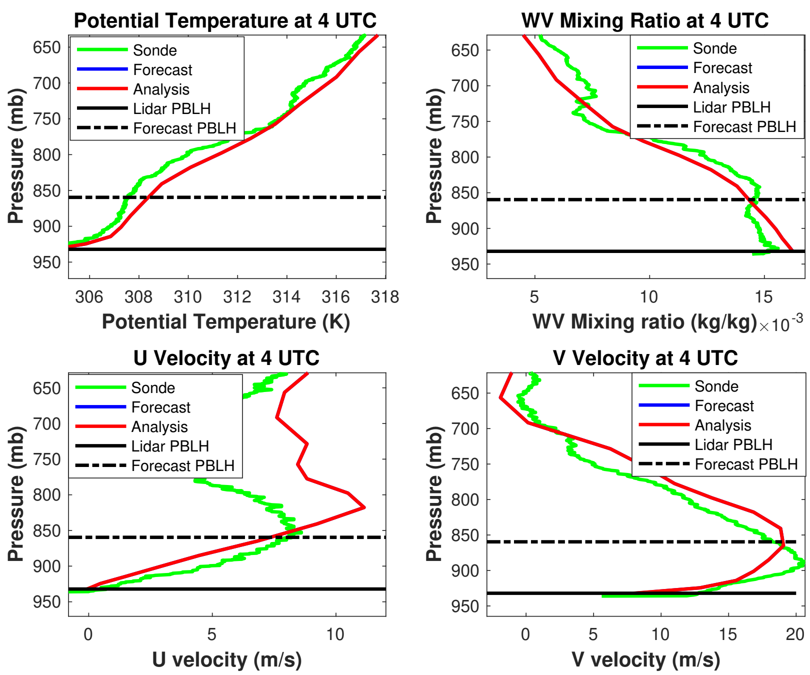

Figure 4. Profiles from ~~sonde~~ radiosonde (green), forecast (blue) and analysis (red) for potential temperature (upper left), water vapor mixing ratio (upper right), u-velocity (lower left) and v-velocity (lower right) at 4 UTC, July 11, 2015 in Greensburg, KS. The model uses the MYJ physics parameterization.

The increasing differences between ~~the~~ PBLH and profile forecasts from early morning to late afternoon only partly explain the much larger impact of the assimilation at 22 UTC. We can also analyze this by plotting the error covariance between PBLH and each of the state variables, seen in Figure **??** at different times during the day. The covariance with temperature ~~(a)~~ is always positive, and grows by a factor of 4 by late afternoon near the surface. The covariance with WV is mostly negative and grows by roughly a factor of 5, while the covariance with the two components of velocity oscillate between

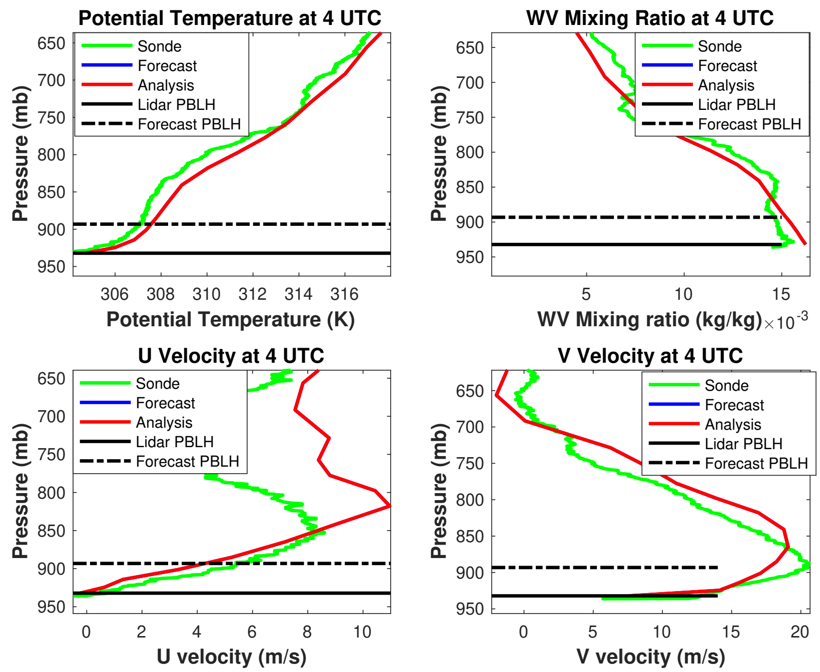

Figure 5. Same as figure **??** except using MYNN model.

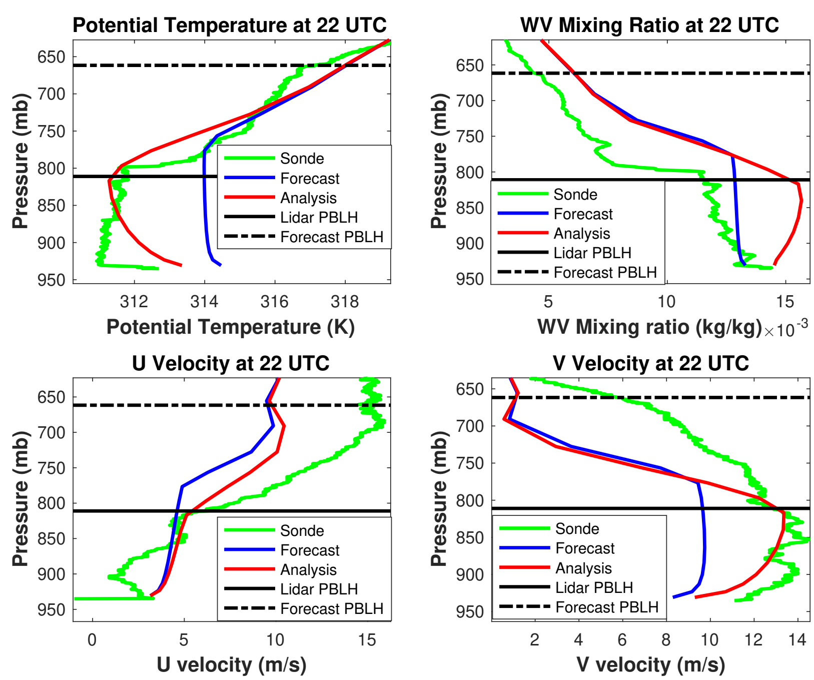

Figure 6. Same as figure **??** except using except at time 22 UTC.

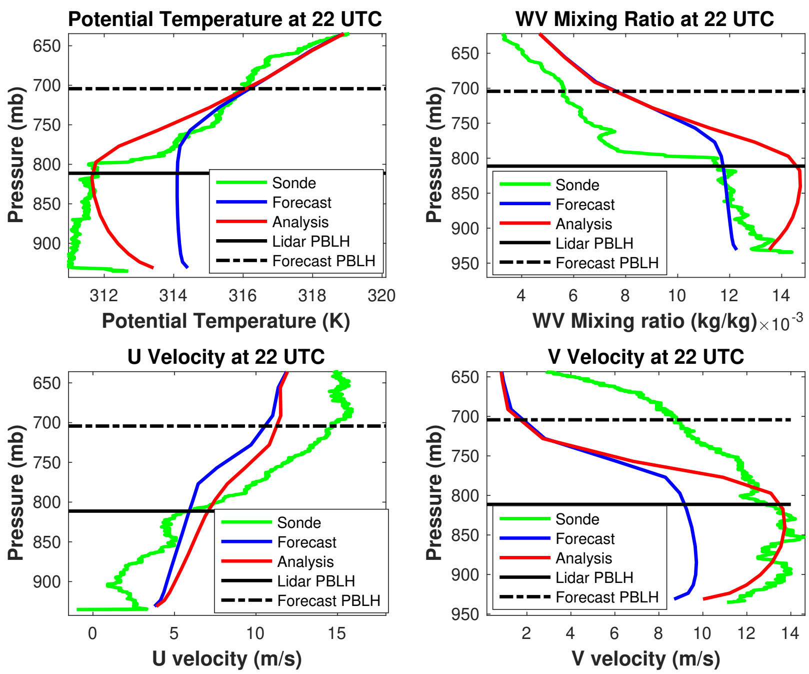

Figure 7. Same as figure **??** except using MYNN model.

positive and negative and shows less consistent growth. Thus, the ~~most significant~~ largest impact of assimilation ~~to~~ on temperature and moisture ~~occur~~ occurs in late afternoon while more limited velocity corrections are largely constrained by the correlations determined by the ensemble of model forecast states.

4 Conclusions

These offline data assimilation experiments indicate that ~~assimilation~~ assimilating ground based lidar backscatter and wind measurements of PBLH into a regional NWP model will likely lead to ~~significant improvements~~ corrections to profiles within the PBL, particulary when this approach is applied to an EnKF assimilation system with cycling. Using two NU-WRF forecasts over a period of one day with different PBL physics models, we show how the state variables, T, WV, U and V can be corrected using an ~~an~~ assimilation system with ensemble based error covariances. During the night and early morning the assimilation has ~~little or no~~ relatively little impact on the state variables, but by late afternoon the temperature field is drawn closer to independent ~~sonde~~ radiosonde measurements. We have shown that the lack of data impact early in the day is the due to the ~~high~~ relatively higher accuracy of the model and lack of correlation between the fore-

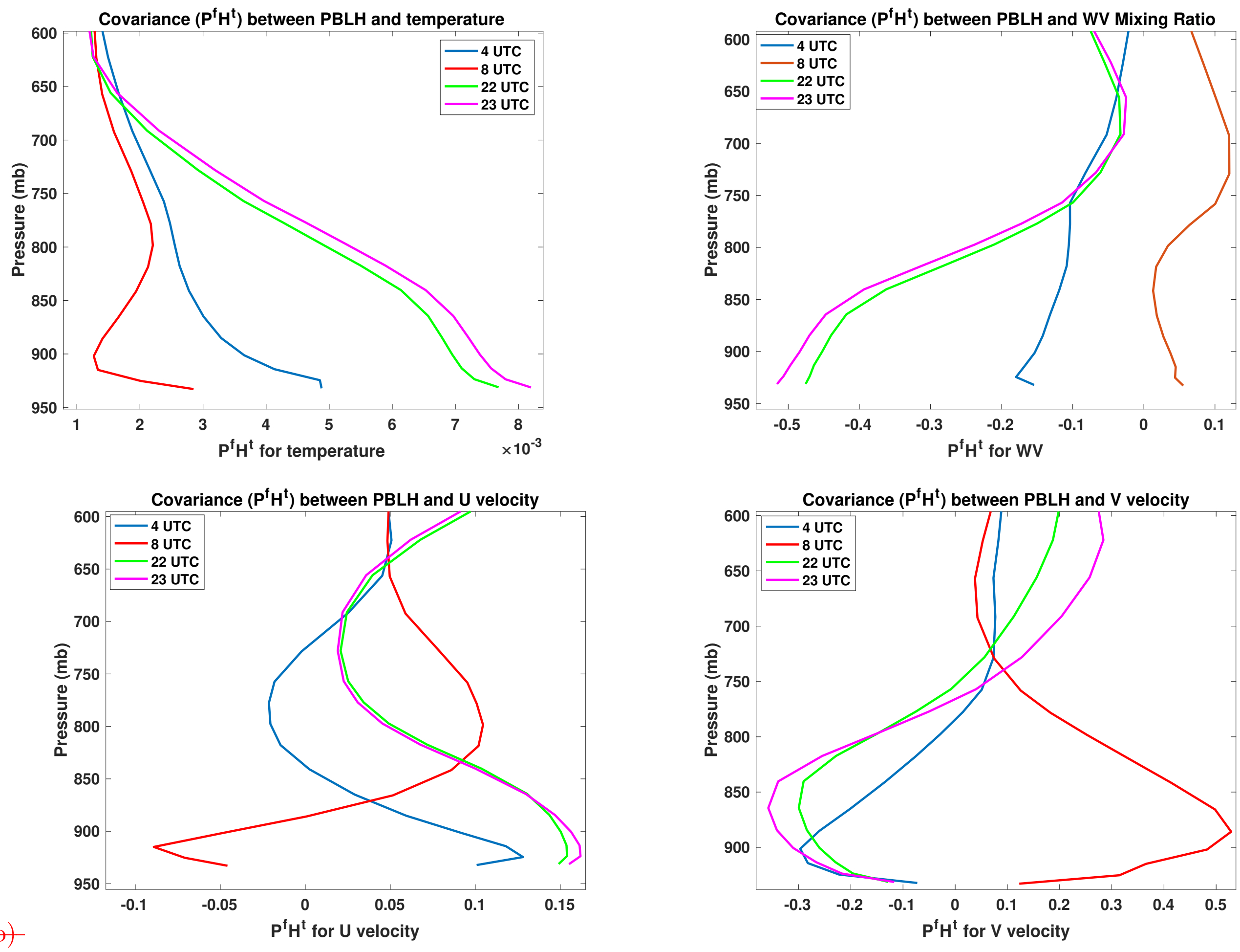

~~(a)~~ ~~(b)~~

~~(b)~~ ~~(c)~~

Figure 8. Covariance $\mathbf{P}^f\mathbf{H}^T$ between PBLH and temperature (~~a~~upper left), water vapor (~~b~~upper right), ~~U-velocity~~ U velocity (~~c~~lower left) and ~~V-velocity~~ V velocity (~~d~~lower right), at times 4, 8, 22 and 23 UTC, for PBL physics model MYHH.

cast PBLH and temperature profiles at that time. Later in the day, when the model is less accurate in predicting the growth of the boundary layer, the data begins to draw the ~~analysis towards the independent sonde~~ analyses mostly toward the independent radiosonde profiles. The assimilation over corrected the water vapor mixing ratio ~~is over corrected~~ in the direction of ~~sonde~~ radiosonde data, and this could likely be tuned in an assimilation system. ~~The assimilation corrected the two velocity components by smaller amounts, but still~~ And it corrected the the V velocity component by a smaller amount, and reduced differences with the ~~sonde profiles~~ radiosonde profiles for the V velocity. These corrections are the result of ensemble computed error covariances between the PBLH and the state variable profiles within the PBL. The results here indicate that this approach ~~could~~ has some potential to be used in a forecast system in a way that that the PBLH observational information could be carried forward in time so as to ~~improve~~ impact the forecast accuracy within the PBL. An additional value of assimilating PBLH is its close connection with the PBL scheme used in the model. The covariances between PBLH and the different state variables are defined through the PBL physics scheme. This has an impact on the corrections made to the profiles within the PBL, which can be used as another way to evaluate the physics parameterizations. For example, the MYJ and MYNN result in analysis profiles that differ, ~~though~~ particularly in WV in the late afternoon. And the differences in reponse to assimilation are an indication of how the two different PBL schemes affect the covariance between PBLH and the state variables. However, a full evaluation would require that the assimilation be implemented into a cycling data assimilation system.

This work is intended only to demonstrate a necessary first step in terms of how ensemble statistics can help to constrain profiles within the PBL by assimilating PBLH observations. A more complete demonstration of this approach will require the construction of an EnKF, and run over many days with a variety of weather patterns, including significantly warmer(cooler) and wetter(drier) days. This is needed to show how the assimilated PBLH observations will impact future forecasts within the PBL. In addition, an EnKf will involve spatial covariances in both horizontal and vertical directions, and will allow for both inflation and horizontal localization. This will enable further tuning of the system to optimize the analysis state relative to the independent radiosonde observations. The PBLH assimilation withn the EnKF framework could be done in any of numerous existing enKF assimilation systems that connect with WRF, including NU-WRf (Lidard-Peters *et al.*, 2015) and WRF-DART (Anderson *et al.*, 2009).

5 Acknowledgments

B. Demoz was funded by National Science Foundation award (AGS-1503563) to the University of Maryland, Baltimore County and through NOAA Cooperative Science Center in Atmospheric Sciences and Meteorology, funded by the Educational Partnership Program at NOAA in collaboration with Howard University.

6 Data Sets

PECAN (`https://data.eol.ucar.edu/master_list/?project=PECAN\verb`) data are archived by NCAR/EOL, which is funded by NSF. The forecast and analysis fields produced for this work are stored at https://alg.umbc.edu/pecan/.

7 Competing Interests

The authors declare that they have no conflict of interest.

8 Author Contributions

Andrew Tangborn built the assimilation system, with input from Jeffrey Anderson on the algorithm. Belay Demoz and Brian Carroll provided the lidar observations. Joseph Santanello provided background information on PBL physics. All of the authors contributed to writing and revising the paper.

9 References

Anderson, J.L., T. Hoar, K. Raeder, H. Liu, N. Collins, R. Torn and A. Arellano (2009), The Data Assimilation Research Testbed: A Community Facility, *Bull. Amer. Met. Soc.*, 90, 1283-1296 doi:10.1175/2009BAMS2618.1.

~~Ao, C.O., T. K. Chan, B. A. Iijima, J.-L. Li, A. J. Mannucci, J. Teixeira, B. Tian, and D. E. Waliser (2008), Planetary boundary layer information from GPS radio occultation measurements, Proceedings of GRAS SAF Workshop on Applications of GPSRO Measurements,~~

ECMWF, Reading, UK. .1in Banks, R. F., J. Tiana-Alsina, F. Rocadenbosch, and J. M. Baldasano (2015) Performance evaluation of the boundary-layer height from lidar and the Weather Research and Forecasting Model at an urban coastal site in the north-east Iberian Peninsula. Bound.-Layer Meteor., 157, 265–292, https://doi.org/ 10.1007/s10546-015-0056-2. .1in Bonin, T.A., B.J. Carroll, R.M. Hardesty, W.A. Brewer, K. Hajney, O.E. Salmon and P.B. Shepson (2018), Doppler Lidar Observations of the Mixing Height in Indianapolis Using an Automated Composite Fuzzy Logic Approach, *J. Atmos. Ocean Tech.*, 35, 473-490.

Brooks, I.M. (2003), Finding Boundary Layer Top: Application of a Wavelet Covariance Transform to Lidar Backscatter Profiles, *J. Atmos. Ocean Tech.*, 20, 1092-1105.

.02in Browning, K. A., and Coauthors (2007), The Convective Storm Initiation Project. , *Bull. Amer. Meteor. Soc.*, 88, 1939–1955, https://doi.org/10.1175/BAMS-88-12-1939.

Carroll, B. J., Demoz, B. B., and Delgado, R. (2019). An overview of low-level jet winds and corresponding mixed layer depths during PECAN. Journal of Geophysical Research: Atmospheres, 124(16), 9141-9160. https://doi.org/10.1029/2019JD030658.

Cohen, A. E., S.M. Cavallo, Coniglio, M. C. Coniglio and H. E. Brook (2015), A Review of Planetary Boundary Layer Parameterization Schemes and Their Sensitivity in Simulating Southeastern U. S. Cold Season Severe Weather Environments, C., G. S. Romine, D. D. Turner, and R. D. Torn, 2019: Impacts of Targeted AERI and Doppler Lidar Wind Retrievals on Short-Term Forecasts of the Initiation and Early Evolution of Thunderstorms. *Wea. Forecat.Mon. Wea. Rev.*, 30, 591-612147, 1149–1170.

.1in Crook, N. A., 1996: Sensitivity of moist convection forced by boundary layer processes to low-level thermodynamic fields. Mon. Wea. Rev., 124, 1767–1785.

.1in Degelia, S. K., X. Wang, and D. J. Stensrud, 2019: An Evaluation of the Impact of Assimilating AERI Retrievals, Kinematic Profilers, Rawinsondes, and Surface Observations on a Forecast of a Nocturnal Convection Initiation Event during the PECAN Field Campaign. *Mon. Wea. Rev.*, 147, 2739–2764.

Delgado, R., Carroll, B. and Demoz, B. (2016). FP2 UMBC Doppler Lidar Line of Sight Wind Data. Version 1.1 [Data set]. UCAR/NCAR - Earth Observing Laboratory. Accessed 29 May 2017. https://doi.org/10.5065/d6q81b4h.

Demoz, B., C. Flamant, T. Weckwerth, D. Whiteman, K. Evans, F. Fabry, P. Di Girolamo, D. Miller, B. Geerts, W. Brown, G. Schwemmer, B. Gentry, W. Feltz, and Z. Wang, 2006: The dryline on 22 May 2002 during IHOP-2002: Convective scale measurements at the profiling site. Mon. Wea. Rev., 134(1), 294-310.

.1in Evensen, G. (2009), *Data assimilation: the ensemble Kalman filter*, Springer.

Geerts, B., and Coauthors, (2017), The 2015 Plains Elevated Convection At Night field project. *Bull. Amer. Meteor. Soc.*, 98, 767–786, https://doi.org/10.1175/BAMS-D-15-00257.1.

Hegarty, J.D., J. Lewis, E.L. McGrath-Spangler, J. Henderson, A.J. Scarino, P. DeCola, R. Ferrare, M. Hicks, R.D. Adams-Selin and E.J. Welton (2018) Analysis of the Planetary Boundary Layer Height during DISCOVER-AQ Baltimore–Washington, D.C., with Lidar and High-Resolution WRF Modeling, *J. Appl. Meteo. Climat.*, 57, 2679-2696.

Hicks, M., D. Atkinson, B. Demoz, K. Vermeesch and R. Delgado (2016), The National Weather Service Ceilometer Planetary Boundary Layer Project, *The 27th International Laser Radar Conference (ILRC 27)*, https://doi.org/10.1051/epjconf/201611915004.

Hicks, M., B. Demoz, K. Vermeesch and D. Atkinson (2019), Intercomparison of Mixing Layer Heights from the National Weather Service Ceilometer Test Sites and Collocated Radiosondes, *J. Atmos. Ocean Tech.*, 36, 129-137.

Holzworth, G.C. (1964), Estimates of mean maximum mixing depths in the contiguous United States, *Mon. Wea. Rev.*, 92, 235-242.

.1in Hong, S.-Y. and H.-L. Pan (1996), Nonlocal boundary layer vertical diffusion in a medium-range forecast model, *Mon. Wea. Rev.*, 124, 2332-2339.

Hong, S.-Y. and H.-L. Pan (1998), Convective Trigger Function for a Mass-Flux Cumulus Parameterization Scheme, *Mon. Wea. Rev*, 126, 2599-2620.

Houtekamer, P.L. and F. Zhang (2016), Review of the Ensemble Kalman Filter for Atmospheric Data Assimilation, *Mon. Wea. Rev.*, 144, 4489-4532.

.1in Hu, J., N. Yussouf, D. D. Turner, T. A. Jones, and X. Wang, 2019: Impact of Ground-Based Remote Sensing Boundary Layer Observations on Short-Term Probabilistic Forecasts of a Tornadic Supercell Event, *Wea. Forecasting*, 34, 1453–1476.

.1in Janjic, Z.I. (1994), The Step-mountain eta coordinate model: Further developments of the convection, viscous sublayer, and turbulence closure, *Mon. Wea. Rev.*, 122, 927-945.

Janjic, Z.I. (2002), Nonsingular Implementation of the Mellor-Yamada Level 2.5 Scheme in the NCEP Meso model (NCEP Office Note No. 437).

T. N. Knepp, J.J. Szykman, R. Long, R. M. Duvall, J. Krug, M. Beaver, K. Cavender, K. Kronmiller, M. Wheeler, R. Delgado, R. Hoff, T. Berkoff, E. Olson, R. Clark, D. Wolfe, D. Van Gilst, D. Neil (2017), Assessment of mixed-layer height estimation from single-wavelength ceilometer profiles, *Atmos. Meas. Tech.*, 10, 3963-3983.

Lothon, M., Lohou, F., Pino, D., Couvreux, F., Pardyjak, E. R., Reuder, J., et al. (2014). The BLLAST field experiment: Boundary-Layer late afternoon and sunset turbulence. Atmospheric Chemistry and Physics, 14(20), 10931–10960. https://doi.org/10.5194/acp-14-10931-2014.

.1in Mellor, G.L. and T. Yamada (1974), A Hierarchy of Turbulence Closure Models for Planetary Boundary Layers, *J. Atmos. Sci.*, 31, 1791-1806.

Mellor, G.L. and T. Yamada (1982), Development of a turbulence closure model for geophysical fluid problems, *Rev. Geophys.*, 20, 851-875.

Nakashini, M. and H. Niino (2009), Development of an improved turbulence closure model for the atmospheric boundary layer, *J. Met. Soc. Japan*, 87, 895-912.

National Research Council (2009), Observing Weather and Climate from the Ground Up: A Nationwide Network of Networks, in: Observing Weather and Climate from the Ground Up: A Nationwide Network of Networks, 1–234, Natl. Academies Press, 2101 Constitution Ave, Washington, DC 20418 USA.

NCAR Technical Note (2012), Thermodynamic Profiling Technologies Workshop Report to the National Science Foundation and the National Weather Service, National Center for Atmospheric Research.

Oke, P.R., G.B. Brassington, D.A. Griffin, and A. Schiller (2010), Ocean data assimilation: a case for ensemble optimal interpolation, *Austr. Meteor.Ocean. J.*, 59, 67-76.

Peters-Lidard, C.A. and Co-authors (2015), Integrated modeling of aerosol, cloud, precipitation and land processes at satellite-resolved scales, *Environ. Mod. Soft.*, 67, 149-159.

Santanello, J.A. and Co-authors (2018), Land–Atmosphere Interactions: The LoCo Perspective, *Bull. Amer. Meteor. Soc*, https://doi.org/10.1175/BAMS-D-17-0001.1.

Santanello, J.A.,, S.Q. Zhang, D.D. Turner, P. Lawston, and W.G. Blumberg, PBL Thermodynamic Profile Assimilation and Impacts on Land-Atmosphere Coupling, AGU Fall Meeting, San Francisco, CA, Dec. 9-13, 2019.

~~Tucker, S.C., S.J. Senff, A.~~Wulfmeyer, V., R.M. ~~Weickmann, W.A. Brewer, R.M.Banta, S. P. Sandberg,~~ Hardesty, D.~~C. Law and R. M. Hardesty (2009), Doppler Lidar Estimation of Mixing Height Using Turbulence, Shear, and Aerosol Profiles~~D. Turner, A. Behrendt, M.P. Cadeddu, P. Di Girolamo, P. Schlussel, J.Van Baelen and F. Zus (2015), A review of the remote sensing of lower tropospheric thermodynamic profiles and its indispensable role for the understanding and the simulation of water and energy cycles, ~~*J. Atmos.Ocean Tech.*~~*Rev. Geophys.*, ~~26, 673-688~~https://doi.org/10.1002/2014RG000476.